

Nonlinear Probabilistic Constellation Shaping with Sequence Selection

Stella Civelli, *Member, IEEE*, Enrico Forestieri, *Senior Member, IEEE*, and
Marco Secondini, *Senior Member, IEEE*

Abstract—Probabilistic shaping is, nowadays, a pragmatic and popular approach to improve the performance of coherent optical fiber communication systems. In the linear regime, the potential of probabilistic shaping in terms of shaping gain and rate granularity is well known, and its practical implementation has been mostly mastered. In the nonlinear regime, the advantages offered by probabilistic shaping remain not only valid, but might also increase thanks to the appealing opportunity to use the same technique to mitigate nonlinear effects and obtain an additional nonlinear shaping gain. Unfortunately, despite the recent research efforts, the optimization of conventional shaping techniques, such as probabilistic amplitude shaping (PAS), yields a relevant nonlinear shaping gain only in particular scenarios of limited practical interest, e.g., in the absence of carrier phase recovery. Recently, a more theoretical approach, referred to as sequence selection, has been proposed to understand the performance and limitation of nonlinear constellation shaping. Sequence selection shapes the distribution of the transmitted symbols by selecting or discarding the sequences generated by a certain source according to a metric that measures their *quality*. In this manuscript, after a brief review of *conventional* probabilistic shaping, we use sequence selection to investigate through simulations the potential, opportunities, and challenges offered by nonlinear probabilistic shaping. First, we show that ideal sequence selection is able to provide up to 0.13 bit/s/Hz additional gain with respect to PAS with an optimized blocklength. However, this additional gain is obtained only if the selection metric accounts for the signs of the symbols, ruling out the possibility of using one of the simple recently proposed sign-independent metrics. We also show that, while the signs must be known to compute the selection metric, there is no need to shape them, since nearly the same gain can be obtained by properly selecting the amplitudes (with a sign-dependent metric) and leaving the signs uniform i.i.d. Furthermore, we show that the selection depends in a non-critical way on the symbol rate and link length: the sequences selected for a certain scenario still provide a relevant gain if the link length or baud rate are modified (within a reasonable range). Then, we analyze and compare several practical implementations of sequence selection by taking into account interaction with forward error correction (FEC), information loss due to selection, and complexity. Overall, we conclude that the single block and the multi block FEC-independent bit scrambling are the best options for the practical implementation of sequence selection, with a gain up to 0.08 bit/s/Hz. The main challenge and limitation to their practical implementation remains the evaluation of the metric, whose complexity is currently too high. Finally, we show that the nonlinear shaping gain provided by sequence selection persists when carrier phase recovery is included, in contrast to

the nonlinear shaping gain offered by optimizing the blocklength of conventional PAS techniques.

Index Terms—Optical fiber communication, nonlinear fiber channel, probabilistic shaping.

I. INTRODUCTION

Since Shannon work in 1948, it is well known that the capacity of an additive white Gaussian noise (AWGN) channel can be theoretically achieved by mapping information to i.i.d. Gaussian input symbols [3], [4]. However, for practical reasons, typical modulation schemes map information to i.i.d. symbols drawn from a discrete modulation alphabet with uniform distribution, such as the simple on-off keying employed by the first generations of optical fiber systems, or more complex square M -ary quadrature amplitude modulations (QAM) constellations employed by more recent optical systems based on coherent detection, in which $m = \log_2(M)$ bits are Gray-mapped to each QAM symbol.

The idea of approaching the Gaussian distribution with discrete constellations has been discussed since the early 1990s [5], [6], but only recently this concept gained considerable attention. Nowadays, this strategy is known as constellation shaping and is a pragmatic approach to improve the performance of communication systems. In particular, probabilistic constellation shaping, or probabilistic shaping in short, consists in mapping information bits on discrete square QAM constellations with a desired probability distribution, chosen such as to approach a Gaussian distribution [7]–[9]. In a nutshell, one decides to reduce the average energy per symbol by using lower-energy symbols more frequently than higher energy ones. The benefit obtained in terms of energy efficiency is partly paid in terms of spectral efficiency: the redundancy of the source is increased (its entropy decreased), and less than m bits can be mapped to each symbol. The best trade-off between energy and spectral efficiency is obtained with a Maxwell–Boltzmann (MB) distribution, which, compared to uniform QAM, allows to improve the performance of the system by either obtaining the same information rate with a smaller signal-noise ratio (SNR), or by improving the information rate for a given SNR, closely approaching channel capacity. The way to map uniform i.i.d. information bits to MB-distributed symbols, and to combine shaping with forward error correction (FEC) has been deeply investigated in the last years [7], [8], [10]–[13], and still is an active research topic nowadays.

Unfortunately, the optimal distribution for a *nonlinear* fiber-optic channel is still unknown and, most likely, not Gaussian

S. Civelli is with the CNR-IEIT, Pisa, Italy. S. Civelli, E. Forestieri, and M. Secondini are with the Institute of Communication, Information and Perception Technologies, Scuola Superiore Sant’Anna, Pisa, Italy. E. Forestieri and M. Secondini are with the National Laboratory of Photonic Networks, CNIT, Pisa, Italy. Email: stella.civelli@cnr.it.

This paper was presented in part at the Optical Communication Conference (OFC), San Diego (CA), March 5-9, 2023. [1], [2].

[14]. For this reason, in the recent years, a lot of effort has been devoted to tailoring probabilistic shaping to the nonlinear fiber-optic channel, trying to obtain an additional nonlinear gain on top of the linear shaping gain [15]–[17]. Indeed, it was recently shown that it is possible to further improve the performance of a system beyond that achievable by merely tailoring *conventional* shaping techniques—developed for the linear channel—to the nonlinear fiber channel. In particular, the *sequence selection* approach extends the conventional concept of probabilistic shaping by automatically optimizing the source according to a proper metric that measures the performance over a given channel. Even in this case, the selection reduces the information rate of the source, trading it for a higher robustness to nonlinear effects, with an overall improvement of system performance [18], [19].

In this paper, after a brief review of *conventional* probabilistic shaping in the linear and nonlinear regimes, we discuss the sequence selection concept, providing interesting bounds for the performance in the nonlinear regime. We discuss the role of the signs of the transmitted symbols, which are irrelevant in conventional probabilistic amplitude shaping (PAS) but become fundamental for the nonlinear channel, and show that a proper selection metric must account for the signs. Next, we propose and discuss the implementation of nonlinear probabilistic shaping techniques based on sequence selection, in particular considering the interaction with forward error correction (FEC) and carrier phase recovery (CPR), and considering different shaping and concatenation strategies.

The manuscript is organized as follows. Section II describes the system used for performance assessment in our simulations, while Section III briefly discusses linear probabilistic shaping. Next, Section IV addresses nonlinear probabilistic shaping, focusing on (i) the performance of conventional shaping in the nonlinear regime, (ii) the sequence selection approach, (iii) the practical implementation of sequence selection, (iv) the performance of different sequence selection approaches, and (v) the interaction with carrier phase recovery. Finally, Section V draws the conclusion.

II. SYSTEM DESCRIPTION

The system setup is as follows [1], [2]. We consider a dual polarization wavelength division multiplexing (WDM) signal with 5×46.5 GBd channels and 50 GHz spacing. The modulation format is dual polarization 64-QAM with probabilistic shaping and root-raised-cosine supporting pulse with rolloff 0.05. As a benchmark, and as a starting point (referred to as unbiased source) for sequence selection, we consider probabilistic amplitude shaping (PAS) with rate $R_{4D} = 9.2$ bit/4D (equivalent to $R_{DM} = 1.3$ bit/amplitude), implemented with the serial mapping for quadratures and polarizations [20]. The signal is sent into a link composed of 30×80 km spans of single mode fiber (SMF) with erbium-doped fiber amplifiers (EDFAs) with noise figure 5 dB. At the receiver side, after demultiplexing, the central channel undergoes electronic dispersion compensation, matched filtering, symbol time sampling, and mean phase rotation compensation. Finally, the achievable information rate (AIR) is evaluated as

the generalized mutual information (GMI), which represents the information rate that can be achieved assuming ideal FEC and bit-wise mismatched decoding under the bit metric decoding [21], [22]. The performance is given in terms of spectral efficiency (SE) in bit/s/Hz, as $SE = 46.5/50 \cdot \text{AIR}$.

III. PROBABILISTIC CONSTELLATION SHAPING

Probabilistic constellation shaping—often simply referred to as probabilistic shaping—denotes the way of mapping information bits onto the symbols of a conventional M -QAM constellation such that they turn out having a *desired* prior probability. This is usually done to approximate the capacity-achieving distribution and improve system performance. In the case of an additive white Gaussian noise (AWGN) channel with *continuous* inputs, the capacity-achieving distribution is Gaussian. On the other hand, when the inputs are constrained on a given constellation of symbols $\mathcal{S} = \{\mathbf{s}_1, \mathbf{s}_2, \dots\}$, an approximately optimal distribution is the Maxwell–Boltzmann (MB) distribution [6]¹

$$p(\mathbf{s}) = \exp(-\lambda \|\mathbf{s}\|^2) / \sum_{\mathbf{s}_k \in \mathcal{S}} \exp(-\lambda \|\mathbf{s}_k\|^2) \quad (1)$$

where $\|\mathbf{s}_k\|^2$ is the energy of the symbol \mathbf{s}_k , and $\lambda \geq 0$ is a parameter that characterizes the distribution and determines the trade-off between bit rate and mean energy per symbol.

In the past years, research has focused on the design of practical approaches for the implementation of probabilistic shaping, leading in particular to the development of the widely deployed probabilistic amplitude shaping (PAS) technique [7], [8]. The key idea of PAS is that of achieving probabilistic shaping by concatenating a fixed-to-fixed distribution matcher (DM) to shape the probability distribution of the amplitudes, and a systematic binary encoder for forward error correction (FEC), whose parity bits (possibly together with other information bits) are mapped to the signs. The DM maps k information bits (i.i.d. with uniform probability) to N_{DM} *shaped* amplitudes from the alphabet $\{1, 3, \dots, 2M_{DM} - 1\}$ with a desired distribution and should be invertible.² The reverse-concatenation scheme ensures that, at the receiver side, FEC decoding can be performed before inverting the DM to demap the information bits from the amplitude, so that the DM inversion is not affected by error propagation and no iterations between demapper and decoder are required. At the same time, the mapping of parity bits on signs ensure that the distribution of the amplitudes is not altered by the FEC, while the distribution of the signs remains uniform (as required by (1)).

The rate of the DM R_{DM} is the amount of bits that are encoded on average on each amplitude, and equals k/N_{DM} .³ However, a practical DM with finite block length N is affected

¹The MB distribution maximizes the entropy for a given constellation and mean energy per symbol [23], and closely approach the capacity for a given constellation and SNR.

²Sometime, it is useful to see the output of the DM in terms of bits, simply considering a corresponding binary representation of the amplitudes with $\lceil \log_2 M_{DM} \rceil$ bits.

³The rate $R_{DM} = k/N_{DM}$ on the DM with an alphabet of M_{DM} positive amplitudes corresponds to the rate $R_{4D} = 4(R_{DM} + 1)$ in bit/4D on a dual polarization M -ary QAM constellation with $M = 4M_{DM}^2$.

by a *rate loss*, i.e., it works at a rate that is slightly lower than the maximal rate (entropy) at which information could be ideally mapped to i.i.d. variables with the same distribution.⁴ For a given constellation size and block length N , the minimum rate loss is obtained with sphere shaping (SpSh), which consists in using the 2^k sequences of length N with minimum energy. Moreover, increasing the block length results in a smaller rate loss. In practice, a DM with a reasonably low rate loss requires a long block length (typically, hundreds of symbols), making its implementation based on a single look-up-table (LUT) unfeasible. Finding a good trade-off between rate loss and implementation complexity is a key aspect in the design of DMs.⁵

Different techniques for the implementation of DMs have been proposed in the past years, including the enumerative sphere shaping (ESS) and its variations [24]–[26]; the constant composition distribution matcher (CCDM) and its variations [10], [22]; and the hierarchical DM (HiDM), which, using multiple DM layers (each based, for instance, on ESS, CCDM, or even LUTs), achieves a lower rate loss compared to the equivalent-complexity single-layer DM [12], [13], [27]. We refer to [20] and references therein for more details about DM implementations.

As an example, the rate loss of SpSh and CCDM is shown in Fig. 1 as a function of the DM block length N_{DM} for a rate of $R_{\text{DM}} \approx 1.3$ bits/amplitude⁶. The figure also shows the rate loss of a LUT-based 6-layer HiDM structure with a slightly larger rate $R_{\text{DM}} = 1.3164$ bits/amplitude and characterized by the following LUT parameters per each layer: output length (8, 2, 2, 2, 2, 2), number of input bits (6, 5, 4, 4, 4, 9), output alphabet order (4, 64, ..., 64). The memory required to save and store the LUTs of this HiDM is only 133 kbit, while the number of operations required for the encoding and decoding is negligible. In the following we will consider the three different DMs highlighted in Fig. 1: the SpSh with block length 256, the CCDM with block length 1024, and the already mentioned HiDM. The CCDM and SpSh have approximately the same rate loss but different block length (i.e., similar linear performance but different nonlinear performance, as shown in the next section) and a non-negligible complexity. On the other hand, HiDM has the same blocklength as SpSh but higher rate loss and almost negligible complexity.

IV. NONLINEAR PROBABILISTIC CONSTELLATION SHAPING

Given the success of PAS in the linear regime, research has recently been directed towards the possibility of using PAS also for nonlinearity mitigation and compensation. In this context, the additional gain (on top of the linear shaping gain) provided by PAS in the nonlinear regime is often referred to

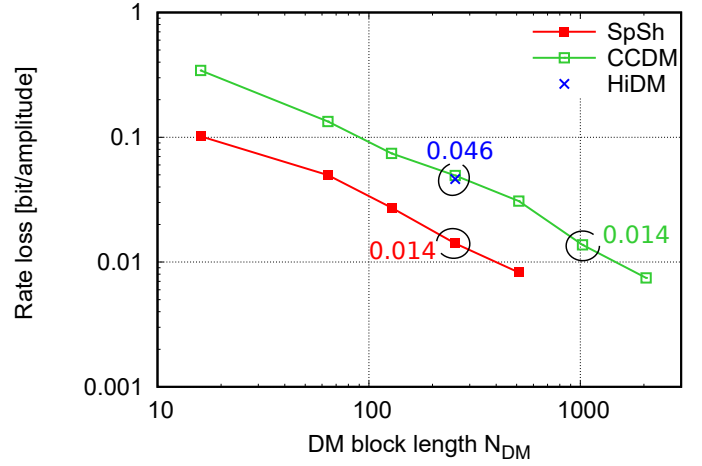


Figure 1. Rate loss versus block length.

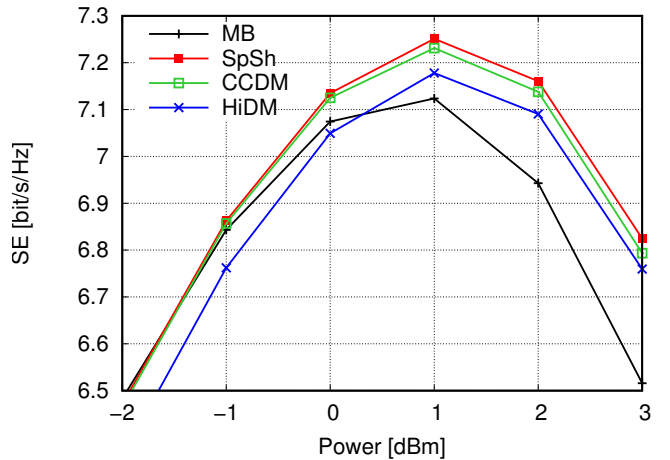


Figure 2. SE versus power with conventional DMs.

as nonlinear shaping gain. In this Section, we first discuss the performance of conventional DMs—i.e., DMs that are designed to implement PAS and optimize its performance in linear regime—in the nonlinear regime and briefly mention some metrics proposed for performance prediction. Next, we describe the sequence selection technique and compute the achievable performance with different flavors of sequence selection. Finally, we propose different implementations of sequence selection, highlighting the main advantages and disadvantages and showing their performance. Finally, we analyze the interaction of sequence selection and carrier phase recovery.

A. Nonlinear Performance of Conventional DM

The performance of ideal PAS (i.e., with i.i.d. MB-distributed symbols) in the nonlinear regime has been investigated in [16], showing that even if the MB distribution is no longer optimal in this case, a full numerical optimization of the target distribution in a 1D (independently per each quadrature component) or 2D (jointly for the in-phase and quadrature components) space does not yield any performance improvement. On the other hand, it has been shown that, in the

⁴Furthermore, with a finite-block-length DM one may not be able to exactly match the desired distribution, but only to approximate it.

⁵However, a low rate loss is not a sufficient condition for good performance, since also the energy loss should be considered. For example, given $\mathcal{S} = \{1, 3\}$, $p(1) = 0.25$ and $p(3) = 0.75$ provides the same entropy of $p(1) = 0.75$ and $p(3) = 0.25$ but with significantly different energy [13].

⁶The actual rate R_{DM} is an approximation of 1.3, since it should be a ratio of two integer numbers. In particular, we select $R_{\text{DM}} = \lfloor 1.3N_{\text{DM}} \rfloor / N_{\text{DM}}$.

nonlinear regime, non-ideal PAS based on short-block-length DMs (e.g., SpSh and CCDM) provides an additional nonlinear shaping gain compared to ideal PAS [15], [28], [29]. Indeed, while increasing the block length of these DMs reduces the rate loss and improves the linear performance,⁷ using a shorter block length reduces the amplitude (energy) fluctuations in the transmitted signal and induces less nonlinear interference [30]. The optimal block length and performance are obtained as a trade-off between these two effects and depend not only on the considered scenario, but also on the specific DM implementation. SpSh has better linear performance with respect to CCDM, band-limited ESS [31], Kurtosis limited ESS [32], and single-shell mapping [20], but has more energy variations and a larger Kurtosis, which are responsible to generate part of the nonlinear interference. Despite this, it was shown that SpSh is able to achieve the largest nonlinear shaping gain, because its lower rate loss allows to improve the linear performance and to use a shorter block length [20]. In the past years, some metrics have been introduced to understand and predict the performance of PAS in the nonlinear regime. With small differences, the energy dispersion index (EDI) [33], the exponentially weighted EDI [34], the Kurtosis [17], and the lowpass-filtered symbol-amplitude sequence (LSAS) [35] have been shown to predict the nonlinear interference in the system and the received signal-noise ratio (SNR). All these metrics accounts only for the energy of the symbols, i.e., they depend only on their amplitudes and not on their signs.

The nonlinear behavior of SpSh, CCDM, and HiDM is shown in Fig. 2 and compared with i.i.d. MB symbols. The figure shows that in the linear regime, the best performance is obtained with MB symbols, closely followed by SpSh and CCDM, while the HiDM has the worst performance. This strictly follows the behaviour in Fig. 1. Conversely, in the nonlinear regime, SpSh achieves the best performance, and i.i.d. MB symbols the worst. The HiDM approaches SpSh and CCDM for increasing power.

However, the performance improvement obtained by employing short-block-length DMs becomes nearly irrelevant when carrier phase recovery (CPR) is included in the system, as in all practical systems. Indeed, we have shown that also CPR mitigates some nonlinear interference—in fact, the same nonlinear interference that is avoided by reducing the PAS blocklength—improving the performance of all DMs and hiding the nonlinear shaping gain provided by short block length PAS in many practical scenarios [20]. This behaviour is predicted by the nonlinear phase noise (NPN) metric, which, differently from EDI, Kurtosis, and LSAS, allows to account also for the impact of CPR [20].

B. Sequence Selection

Sequence selection was proposed for the first time in [18] as a novel technique to understand the ultimate potential and limitations of nonlinear shaping. Combined with an improved detection metric, sequence selection has been shown to provide a new lower bound to the capacity of the nonlinear optical fiber

⁷For $N \rightarrow \infty$, both SpSh and CCDM converge to an ideal source of i.i.d. MB-distributed symbols, and their rate loss vanishes.

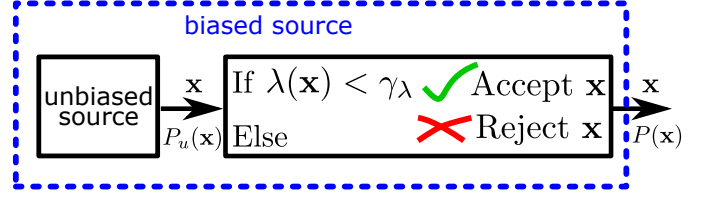


Figure 3. Sequence selection.

channel [19]. In a nutshell, sequence selection uses only *good* sequences for information transmission, rejecting all others.

Sequence selection is implemented as a rejection sampling algorithm, as in Fig. 3. An unbiased source generates sequences \mathbf{x} of n 4D symbols, with unbiased probability $p_u(\mathbf{x})$, e.g., with uniform distribution or probabilistic shaping. Given \mathbf{x} , a selection metric (or cost function) $\lambda(\mathbf{x})$ is evaluated, and the sequence is accepted and used for transmission if the metric is below a certain threshold γ_λ . Note that in this case both amplitudes and signs are shaped by the selection. The acceptance rate η is estimated as $\eta = N_a/N_p$, with N_a and N_p being the number of accepted and proposed sequences. The use of the biased source in Fig. 3 induces a loss in information, because a smaller set of all possible sequences is used. This loss is accounted for in the achievable information rate (AIR) as

$$\text{AIR} = \text{AIR}_u - \frac{1}{n} \log_2 \frac{N_p}{N_a} \text{ [bits/4D]} \quad (2)$$

where AIR_u is the AIR according to the unbiased source $p_u(\mathbf{x})$ and the second term is the loss due to selection [19, Eq. (8)]. The effectiveness of sequence selection depends on the selection metric $\lambda(\mathbf{x})$, as well as on the unbiased distribution $p_u(\mathbf{x})$, on the sequence length n , and on the acceptance rate η . In our case, to assess the potential of nonlinear shaping and understand how much can be achieved, we use the average NLI metric described in [19, Sec. V.C], which estimates the NLI in a single-channel noiseless scenario, averaging over the impact of adjacent sequences to account for inter-block NLI. For more details about sequence selection, we refer to [19]. We refer to this as *ideal* sequence selection, where ideal refers to the fact that this is not a practically implementable transmission technique (in contrast with more practical schemes described later).

To understand how the potential of sequence selection depends on the adopted metric, we consider three different cases. In the first case, which we refer to as ideal sequence selection with *shaped* signs, we assume that both the amplitudes and signs are shaped according to the average NLI metric $\lambda(\mathbf{x})$ described above. In the second case, which we refer to as ideal sequence selection with *unshaped* and *unknown* signs, we assume that only the amplitudes are shaped (as in PAS), and that the metric $\lambda(\mathbf{x})$ is independent of the signs of the symbols in \mathbf{x} . This is the case when a simple metric is adopted (e.g., EDI, NPN, LSAS, or Kurtosis) and/or when the signs are determined by the FEC after the selection procedure, as in the reverse concatenation scheme of PAS. As an ideal metric for this case we adopt the average NLI metric described above, further averaging over the possible signs of the symbols in \mathbf{x} .

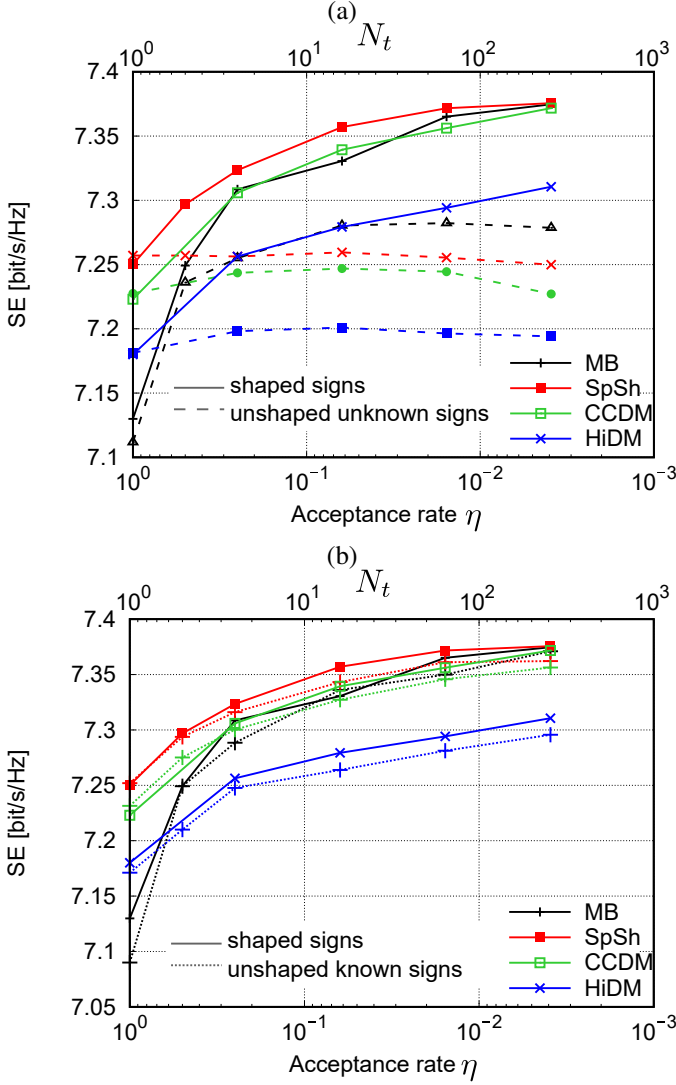


Figure 4. Optimal SE versus acceptance rate η with ideal sequence selection with (a) shaped signs (solid) and unshaped unknown signs (dashed), and (b) shaped signs (solid) and unshaped known signs (dotted).

Finally, in the third case, we consider the intermediate scenario of ideal sequence selection with *unshaped* and *known* signs, where the signs of the symbols are known and used to compute the metric $\lambda(\mathbf{x})$ as in the first case, but they are fixed a priori and cannot be modified by the selection procedure.

Figures 4(a)-(b) show the performance of the system with different sequence selection strategies as a function of the acceptance rate η , with $N_p = 36864$ and at the optimal power $P = 1$ dBm. Furthermore, in order to ease comparison with the results in the next sections, the quantity $N_t = N_p/N_a$ is reported on the top axis. As the unbiased source, we consider either i.i.d. MB-distributed symbols, which yield the best performance in the linear regime with no rate loss, or the three practical DMs whose rate loss is highlighted in Fig. 1. Obviously, when the acceptance rate is 100%, i.e., sequence selection is not applied, SpSh, HiDM, CCDDM, and MB have the same performance shown in Fig. 2 (at optimal launch power), regardless of the shaping strategy adopted on the signs (but for minor statistical fluctuations). When sequence selection

is performed on both amplitudes and signs, the performance of all PAS techniques improves, as shown by the solid line curves in Figs. 4(a)-(b). Interestingly, even though the four PAS strategies have different performance without sequence selection, three of them (SpSh, CCDDM, and MB) achieve nearly the same peak performance $SE = 7.38$ bit/s/Hz when the acceptance rate is reduced to the lowest tested value $\eta = 3.9 \cdot 10^{-3}$, with gains of 0.13 bit/s/Hz, 0.16 bit/s/Hz, and 0.25 bit/s/Hz, compared to their respective values without sequence selection. This is explained by the fact that the initial gap between the three techniques depends on their different blocklength (256, 1024, and virtually infinite, respectively), where shorter values mean less intensity fluctuations and, consequently, less NLI. In this case, the sequence selection procedure automatically controls also the intensity fluctuations of the selected sequences, closing the performance gap between them. On the other hand, HiDM has the same blocklength as SpSh but higher rate loss (see Fig. 1). This means that its intensity fluctuations are already quite limited (as in SpSh), so that it gets from sequence selection nearly the same gain as SpSh, while the initial performance gap, which in this case is due to the rate loss, cannot be recovered by sequence selection.

Clearly the signs of the symbols in \mathbf{x} are irrelevant to determine the intensity fluctuations that cause NLI. This means that the portion of the gain of sequence selection that can be ascribed to the reduction of intensity fluctuations should be equally achieved by shaping only the amplitudes with a sign-independent metric. This is confirmed by the dashed-line curves in Fig. 4(a), which show that sequence selection with unshaped unknown signs provides a relevant gain only with MB (recovering the performance gap with respect to SpSh), an almost negligible gain with CCDDM and HiDM, and no gain with SpSh. In practice, Fig. 4(a) shows that an effective sequence selection strategy requires the use of a sign-dependent selection metric, while no relevant improvements can be expected with sign-independent metrics (e.g., the EDI, LSAS, NPN, and Kurtosis), unless the unbiased source (before selection) is not properly optimized to remove intensity fluctuations.⁸ This is probably not a sufficient reason to use sequence selection with a sign-independent metric, given that the same performance can be achieved (with significantly lower complexity) by optimizing the PAS blocklength and/or including CPR. On the other hand, Fig. 4(b) shows that sequence selection with unshaped but known signs (dotted-line curves) achieves almost the same performance as sequence selection with shaped signs. This means that shaping the signs is not really necessary. They can remain uniform i.i.d. and it is sufficient to account for them when selecting the amplitudes by using a sign-dependent metric. In other words, for a given sequence of signs, there are good and bad amplitude sequences that can be properly selected.

⁸For example, the EDI and LSAS do provide some nonlinear shaping gain when used for a sort of sequence selection in [35]. However the unbiased source employed in [35] (PAS 256QAM and CCDDM with rate $R_{DM} = 2.4$ bit/amplitude and block length 904), is not optimized for nonlinear performance, and a similar gain could be obtained by using SpSh without sequence selection.

An obvious concern is how well the sequences optimized for a given scenario remain valid as the system parameters change. First of all, the optimization does not depend on the launch power, since the adopted NLI selection metric simply scales, with good approximation, with the cube of the power [19], leaving unaltered the sequence ranking. Therefore, we study the dependence of the optimization on other system parameters, namely the link length and the symbol rate. Fig. 6(a) shows the SE versus the number of spans N_{span} at fixed launch power $P = 1$ dBm when sequence selection is not applied (cyan lines), and when sequence selection is applied with two different acceptance rates. In this case, the sequence optimization is done only for $N_{\text{span}} = 30$ and kept fixed for the other values of N_{span} . Obviously, the performance of the system decreases when the link length increases. Interestingly, the gain provided by sequence selection remains nearly constant with N_{span} , despite the sequences being optimized for 30 spans, meaning that the transmitter does not need to know the exact link length and can use the same selection criterion for different lengths. Obviously, when N_{span} decreases, the SE saturates to the maximum value of 8.56 bit/s/Hz, and therefore we do not show the performance in this region. To account for smaller N_{span} , Fig. 6(b) shows the SNR gain (SNR with sequence selection minus SNR without sequence selection) obtained with sequences optimized at $N_{\text{span}} = 30$ (the same in Fig. 6(a), shown with dashed lines) and with sequences optimized at the correct N_{span} value (shown with solid lines). The figure shows that the gain decreases and approaches zero when the sequences optimized for $N_{\text{span}} = 30$ are used for a much smaller link, while the gain achievable with the correct sequences remains almost constant (≈ 0.2 dB and ≈ 0.3 dB with $\eta = 1/64$ and $\eta = 1/256$, respectively). The small improvement in gain when N_{span} increases is probably due to the unavoidable saturation of the SE curves to their maximum value of 8.56 bit/s/Hz when N_{span} decreases (not shown in the figure). On the other hand, 6 shows the SE versus the baud rate R_s . In this case, to keep the overall spectral content unchanged and ensure a fair comparison, we consider d WDM channels with baud rate $R_s = 232.5/d$ GBd, channel spacing $250/d$ GHz, and launch power $P = 3.32 - \log_2 d$ dBm. When the sequences are specifically selected for each given rate, sequence selection provides similar gains for all the considered baud rates, as shown with solid lines. Conversely, when the sequences are selected for a specific rate (e.g., $R_s = 46.5$ GBd with $d = 5$ channels) but used at different rates, the gain has a maximum at this rate and reduces for the other values, as shown with dashed lines. Still, the gain remains relevant even if the baud rate changes significantly.

C. Practical Implementation of Sequence Selection

The sequence selection technique described above serves as a nonlinear equivalent of the MB distribution, allowing to establish the potential and limitations of nonlinear probabilistic shaping. Achieving the AIR calculated with sequence selection requires a practical coded modulation scheme to map information bits on sequence of symbols that have the same statistical properties as those generated by the biased source in

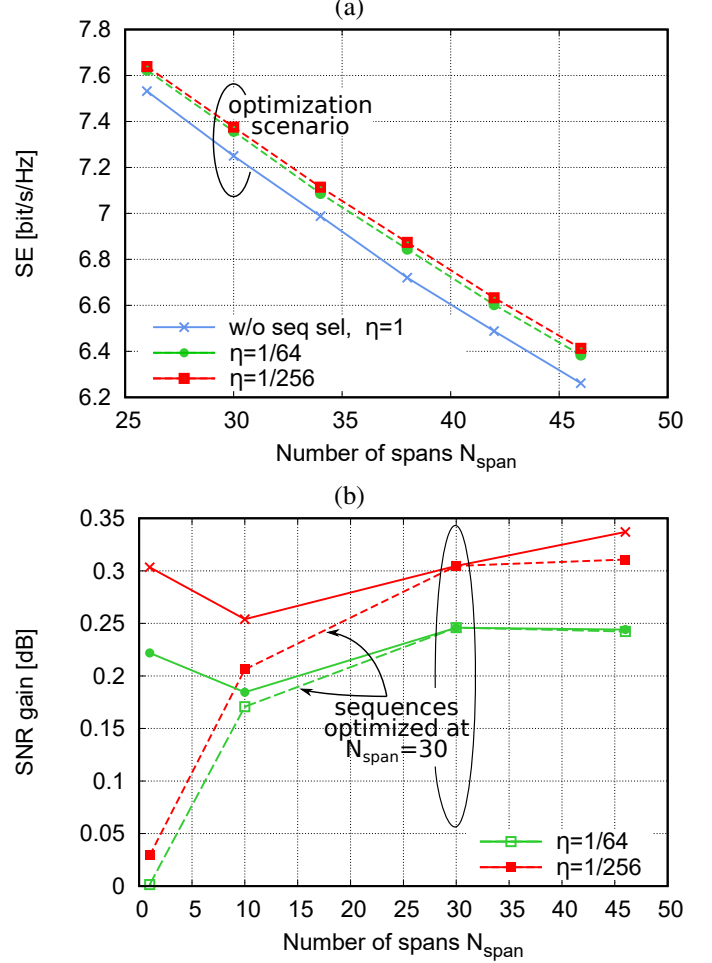


Figure 5. Performance with sequence selection (with shaped signs and SpSh as unbiased source) versus number of spans N_{span} when the sequences are selected for $N_{\text{span}} = 30$ with dashed lines (a) SE, and (b) SNR gain, compared with performance when sequences are optimized for the actual N_{span} with solid lines.

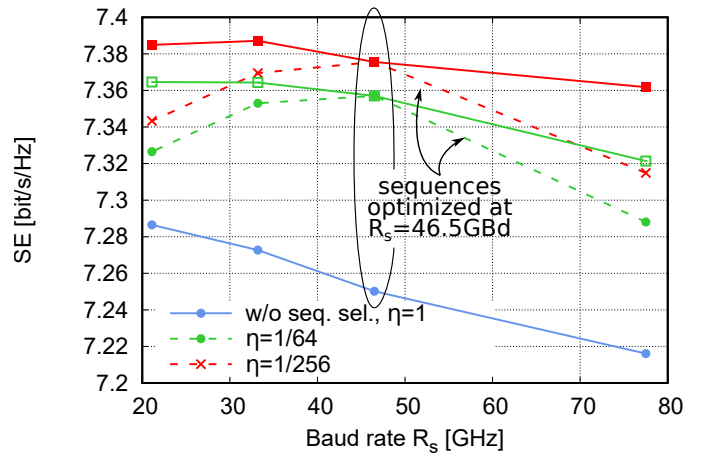


Figure 6. SE with sequence selection (with shaped signs and SpSh as unbiased source) versus baud rate R_s when the sequences are selected for the actual rate (solid) or for $R_s = 46.5$ GBd (dashed).

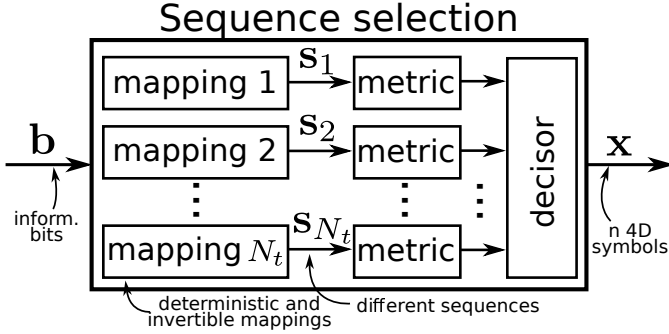


Figure 7. General structure for the practical implementation of sequence selection.

Fig. 3—exactly as the PAS scheme maps information bits on (approximately) i.i.d. MB-distributed symbols [7]. A general scheme for a practical implementation of sequence selection is sketched in Fig. 7. A sequence of information bits \mathbf{b} is mapped to N_t different test sequences of symbols through N_t different mapping rules. The N_t sequences are then compared according to a desired metric, and the *best* sequence \mathbf{x} is selected for transmission. The overall mapping strategy should (i) be invertible, to allow decoding, and (ii) produce *sufficiently* different sequences, emulating the generation of N_t independent sequences. The main difference between ideal sequence selection in Sec. IV-B and its practical implementation is that the first selects sequences with rate η according to a certain threshold γ_λ while the latter selects one sequence out of N_t , without any constraints on its metric—and, therefore, without control over its quality.

To the best of our knowledge, the first attempt to a practical implementation of sequence selection is the list-encoding CCDD structure [36]. Using as a reference Fig. 7, the different sequences are generated by prepending some *flipping* bits to \mathbf{b} and using the CCDD. N_t different combinations of $\log_2 N_t$ flipping bits are used to obtain, at the CCDD output, N_t different sequences. The mapping strategy is easily inverted by using the inverse CCDD and simply discarding the flipping bits. In this case, the sequences are compared according to the EDI. The list-encoding CCDD was later extended to account for different metrics and different shaping techniques [35], [37]. The main drawback of this scheme is that the generation of the sequences is strictly related to the shaping strategy: a DM should be used, the sequence length n should be compatible with the DM block length, and the selection takes into account only the amplitudes (and not the signs).

However, this constraint can be overcome by separating the modulation (which can include or not an initial shaping) and the generation of different sequences, such as in the bit scrambling (BS) sequence selection approach [2]. In this case, given the information bits \mathbf{b} , the N_t sequences are generated by (i) creating N_t different scrambled versions of \mathbf{b} ; (ii) prepending a different combinations of $\log_2 N_t$ pilot bits to each of them (to allow decoding); and (iii) mapping the N_t bit sequences to N_t sequences of symbols according to a desired (shaped or unshaped) modulation format. The BS scheme and other coded modulation schemes with similar characteristics

are described in the next sections.

1) *Bit Scrambling Sequence Selection*: The BS scheme is sketched on the top of Fig. 8 for $N_t = 2$ test sequences, and works as follows [2]. Given a sequence of n_{inf} information bits \mathbf{b} , N_t different sequences are generated, each obtained prepending $n_p = \lceil \log_2 N_t \rceil$ pilot bits to the sequence of bits $\mathbf{t}_k \oplus \mathbf{b}$, with \mathbf{t}_k being a fixed sequence for $k = 1, \dots, N_t$.⁹ For the sake of illustration, in the top of Fig. 8 the first sequence uses the pilot bit 0 and \mathbf{t}_1 is the identity, while the second uses the pilot bit 1 and $\mathbf{t}_2 = \mathbf{t}$. Each bit sequence, of length $n_{\text{inf}} + n_p$, is sent to a conventional PAS block to produce n 4D QAM symbols. The PAS block is the concatenation of DM, FEC with rate c , and QAM encoder, with the following details. Firstly, the sequence of bits is sent to a set of $4n/N_{\text{DM}}$ DMs, each with block length N_{DM} and rate R_{DM} . The set of DMs takes $4nR_{\text{DM}}$ bits to produce $4n$ shaped amplitudes from an alphabet of $\sqrt{M}/2$ elements (corresponding to $4n \log_2(\sqrt{M}/2)$ bits), while the remaining $n_u = n_{\text{inf}} + n_p - 4nR_{\text{DM}}$ bits are left unchanged. The resulting sequences, of $n_{\tilde{\mathbf{b}}} = n_u + 4n \log_2(\sqrt{M}/2)$ bits—indicated as $\tilde{\mathbf{b}}_1$ and $\tilde{\mathbf{b}}_2$ in Fig. 8—are sent to the FEC encoder. The FEC produces $n_{\tilde{\mathbf{b}}}(1-c)/c$ parity bits, which, together with the input $n_{\tilde{\mathbf{b}}}$ bits, generate a sequence of n 4D QAM symbols according to PAS: $4n$ shaped amplitudes (written as $4n \log_2(\sqrt{M}/2)$ bits), and $4n$ signs coming from $n_{\tilde{\mathbf{b}}}(1-c)/c$ parity bits and from the unshaped n_u bits. After some easy calculation it turns out that $n_u = 2n(2 - (1-c) \log_2 M)$, $n_{\tilde{\mathbf{b}}} = 2nc \log_2 M$, and $n_{\text{inf}} = 2n(R_{\text{AD}}/2 - (1-c) \log_2 M) - n_p$.¹⁰ Finally, the metric corresponding to each sequence of n 4D QAM symbols is evaluated, and the sequence with the best metric is transmitted. At the receiver side, QAM demodulation, FEC decoding, and inverse DM are performed as in the standard PAS scheme, and the pilot bits are finally used to descramble the received bits and recover \mathbf{b} .

The main difference with respect to list-encoding CCDD and its variants is that the generation of different sequences is not induced by the DM (hence, combined with PAS and constrained by it), but simply obtained with bit scramblers (xor operations). As a consequence, the length n of the sequences to be selected is not related to the PAS block length (except for the soft requirement that $4n/N_{\text{DM}}$ should be an integer number), and the two lengths can be optimized almost independently. Moreover, the selection process can involve also the sign bits of the sequence, which are not involved in PAS, allowing for higher gains (as shown in Fig. 4).

The main drawback of the BS sequence selection is its complexity, since FEC, DM and metric should be evaluated for each N_t sequence. In particular, the FEC should be performed for each sequence since the parity bits are sent to the signs and depends on the amplitudes. This implies that the number of bits in output from the DMs block, equal to $2nc \log_2 M$, should be compatible with the input length to the FEC. For example, the low-density parity-check (LDPC) codes from

⁹The optimization of the scrambling vectors \mathbf{t}_k might provide additional gain, but it is left for a future work.

¹⁰Note that, indeed, $2n(R_{\text{AD}}/2 - (1-c) \log_2 M)$ is exactly the amount of bits that are encoded on n 4D symbols with PAS, when sequence selection is not used.

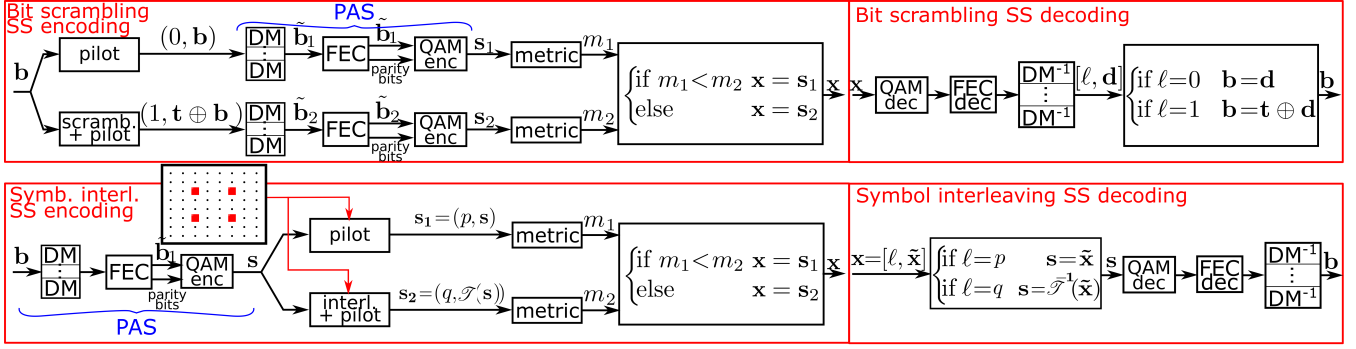


Figure 8. Bit scrambling (BS) and symbol interleaving (SI) sequence selection

DVB-S.2 standard with rate $1/2$ takes in input 32400 bits, and, therefore, requires sequences of length $n = 5400$ if $M = 64$.

2) *Symbol Interleaving Sequence Selection*: The SI approach, sketched on the bottom of Fig. 8 for $N_t = 2$ test sequences, was proposed to overcome some of the drawbacks of BS [2]. The main difference with respect to BS is that the selection process is moved after the cascade of DM, FEC, and QAM encoder—the PAS block. The N_t test sequences are generated by applying different interleavers to the modulated sequence, and adding different pilot symbols to each test sequence—selected from a subset of the employed QAM constellation—to identify the interleaving operation and allow deinterleaving at the receiver. Therefore, the subset of QAM symbols should be large enough to identify the N_t different sequences by using a small number of pilot symbols, but also have a large minimum distance between the symbols to minimize the error probability (given that the pilot symbols are not protected by FEC). In our case, we considered a set of 4 symbols on both polarizations, as shown in the inset in the bottom of Fig. 8, allowing to address up to 16 different sequences with one 4D symbol, and up to 256 with two 4D symbols. With this choice we did not find any error on the pilot symbols during our simulations.

Overall, this approach allows to reduce the complexity by applying the DM and FEC only once, rather than N_t times, and to avoid any constraint on the FEC and sequence selection lengths. However, the pilot symbols are not protected by FEC, and their use induces a higher rate loss compared to the $\lceil \log_2 N_t \rceil$ bits per sequence required by BS. For example, choosing a subset of 4 symbols out of a 64QAM constellation as in our case, one needs $\lceil (\log_2 N_t)/4 \rceil$ 4D pilot symbols, with a loss of $12 \lceil (\log_2 N_t)/4 \rceil$ bits per sequence.¹¹

3) *FEC-Independent BS*: A general approach to solve the issues related to the interaction of FEC in the BS approach is the FEC-independent BS, sketched in Fig. 9. In a nutshell, the FEC-independent BS uses the BS approach (hence without the issues of the SI approach), but moving the FEC *after* the selection process. In this way, the FEC is applied only to the selected sequence (rather than to N_t sequences). Furthermore,

the lengths of DM, sequences, and FEC can be independently selected, since the FEC can be applied on the concatenation of several sequences. In this scheme, the main issue is that of finding a proper way to map the parity bits generated by the FEC on the selected sequence, without altering the particular shaping induced by the selection process. The problem is not simple, since the number of parity bits can be quite large. Given a sequence of n 4D symbols, an M -QAM constellation, and a FEC rate c , the number of parity bits is $2n \log_2 M(1-c)$, and the ratio between the parity bits and the signs bits is $\nu = (1-c) \log_2 M/2$. For example, with $M = 64$: if $c = 2/3$, $\nu = 100\%$, while if $c = 4/5$, $\nu = 60\%$. Possible solutions for the parity bits are discussed below.

The simplest approach is to use a sign-independent metric for the selection and place the parity bits on the signs of the symbols (as in conventional PAS). In this case, the BS and the FEC-independent BS approach are equivalent, since the metric value is not altered by the specific parity bits produced by the FEC, so that they can be determined and mapped to the sequence after the selection process. Unfortunately, this approach is not practically useful, since it does not provide any additional gain with respect to a properly optimized conventional PAS, as shown by the case of ideal sequence selection with unshaped unknown signs in Fig. 4.

A possible approach to use a sign-dependent metric is the single-block FEC-independent BS (SB-BS) scheme sketched in the lower left of Fig. 9. In this case, the sequence of symbols (including their signs) is selected according to the desired sign-dependent metric, but then the parity bits produced by the FEC encoder are mapped to (part of) the signs of the same selected sequence, actually modifying them with respect to the selected ones, hence reducing the accuracy of the selection process. When the FEC rate is small, the percentage of parity bits with respect to the sign bits ν is large (e.g., $c = 2/3$, $\nu = 100\%$) and the method practically reduces to the use of a sign-independent metric (with no expected additional gain with respect to conventional PAS). However, when the FEC rate is larger and ν becomes smaller, part of the sequence is correctly characterized by the metric and the method should provide some gain over the use of a sign-independent metric. The position of the parity bits is discussed in the next Section.

An alternative approach to FEC-independent BS is suggested by the scenario of ideal sequence selection with *un-*

¹¹Furthermore, interleaving $4n/N_{DM} \geq 1$ output DM blocks reduces the nonlinear shaping gain due to short block length DM, thus reducing the overall performance. This requires to use smarter interleaving approaches, for example interleaving the sequence according to independent blocks, each of length N_{DM} .

shaped and *known* signs considered in Section IV-B, which shows that it is not necessary to select (shape) the signs of the sequence, since it is sufficient to know their value when selecting the amplitudes to achieve nearly the same shaping gain. A possible implementation of such a strategy is the multi-block FEC-independent BS (MB-BS) sketched in the lower right of Fig. 9, where the parity bits of each selected sequence are mapped to a fraction ν of the signs of the next sequence (similarly to the *bootstrap* scheme proposed in [38]). In this case, when selecting a certain sequence, these signs are predetermined by the parity bits coming from the previous sequence; they are known and can be used in the computation of the metric, but must be kept fixed during the selection process (the corresponding bits are not scrambled). The main drawback of MB-BS is the latency, since the encoding encompasses several blocks, and the decoding should be performed in reverse order, after the last block has been received.

4) *Performance of Sequence Selection Implementations:* In this Section, the performance of different sequence selection schemes is studied. At the unbiased source, we consider the same four different shaping techniques as in Sec. IV-B. As a metric, we consider the nonlinear interference due to self phase modulation, estimated through a numerically emulated single-channel noiseless propagation of the test sequences. To assess the performance, we evaluate the SE, through the AIR in Eq. (2), recalling that $N_p/N_a = N_t$ when practical implementations of sequence selection are considered. To partially compensate for the loss due to selection, for MB, SpSh, and CCDDM, we increase the PAS rate by the same quantity $\frac{1}{n} \log_2(N_p/N_a)$ in (2). Regarding the HiDM, for the sake of simplicity, we use the HiDM structure in Sec. III for $N_t \leq 16$, while for $N_t > 16$, we increase the number of input bits to each LUT of each layer to (7, 3, 5, 4, 3, 9), to obtain a larger rate equal to 1.3398 bit/amplitude (with negligible difference in rate loss and memory requirements).

Fig. 10 shows the performance of BS sequence selection as a function of the sequence length n^{12} for $N_t = 256$ (solid) and $N_t = 16$ (dashed) tested sequences. When n is too small, sequence selection does not work because the loss induced by selection ($\frac{1}{n} \log_2 N_t$) is large and the impact of adjacent sequences (not considered by the metric) too relevant. On the other hand, when n is increased, sequence selection yields a larger gain, provided that a sufficiently small acceptance rate is considered [19]. The figure shows that a good trade-off between these two effects is obtained with $n = 512$, which will be considered in the following. Note that in the list-encoding CCDDM approach, n is strictly related to N_{DM} and this optimization is not possible.

Figure 11(a) compares the performance of BS sequence selection with that of ideal sequence selection with shaped signs (already shown in Fig. 4), as a function of N_t and for different unbiased sources. While the performance improves with N_t in all cases, the difference between BS and ideal sequence selection is not negligible, meaning that more efficient practical implementations are theoretically possible. The BS

implementation yields a similar SE gain (up to approximately 0.09 bit/s/Hz) with any of the three DMs (SpSh, CCDDM, and HiDM), and a larger gain (about 0.14 bit/s/Hz) with i.i.d. MB symbols, for which it is also able to partly recover the performance gap with respect to the finite-blocklength DMs (as already observed in the ideal case but to a lesser extent).

Fig. 11(b) shows the performance obtained with the SB-BS sequence selection for different parity-to-sign-bit ratios ν (corresponding to different FEC rates c) and two different allocation schemes of the parity bits: *consecutive*, when the parity bits are all mapped to the signs (for both quadratures and polarizations) of the first consecutive symbols of the sequence; and *random*, when they are randomly allocated along the sequence on a fraction ν of the signs. For the sake of comparison, the performance of BS is also reported. As expected, the figure shows that the performance improves as the percentage of parity bit decreases (and the FEC rate consequently increases), and there is no gain when $\nu = 100\%$. Interestingly, placing the parity bits on consecutive symbols provides better performance, meaning that it is better to have a part of the sequence (the one without parity) properly shaped and another part not (the one modified by the parity bits), than having a uniform distribution of modified signs over the whole sequence. In the following, we will consider only the case with consecutive symbols for the SB-BS approach.

Finally, Fig. 11(c) compares the performance of all the sequence selection approaches discussed so far, including MB-BS and SI, considering the SpSh DM in all the cases. Interestingly, the FEC-independent scheme based on the MB-BS approach is able to achieve the same performance as the original BS, independently of the fraction ν of sign bits that are predetermined by the parity bits of the previous block and of their allocation scheme—which are, therefore, not indicated in the legend. This result is in accordance with the behavior shown for ideal sequence selection with unshaped known signs in Section IV-B and implies that FEC can actually be moved after sequence selection (hence reducing the complexity) with no performance penalty, provided that a longer latency can be tolerated. On the other hand, both SB-BS and SI yield a lower SE gain, the former performing approximately as the latter for $c = 4/5$.

D. Interaction of Sequence Selection and Carrier Phase Recovery

The study of the interaction of shortblock-length PAS and carrier phase recovery (CPR) in the nonlinear regime showed that, in the presence of the latter, the nonlinear shaping gain provided by the former vanishes or becomes negligible in most of the scenarios of interest [20], [39]. In fact, CPR, always present in practical coherent systems, can already mitigate some nonlinear effects, possibly making the work done by a specific nonlinear constellation shaping algorithm less effective or even useless. This result pushed the research toward new shaping architectures specifically suited for nonlinearity mitigation, such as sequence selection, and made clear the need to include the effect of CPR in the assessment of their performance.

¹²For the CCDDM, we consider only $n \geq 256$, since $N_{DM} = 1024$.

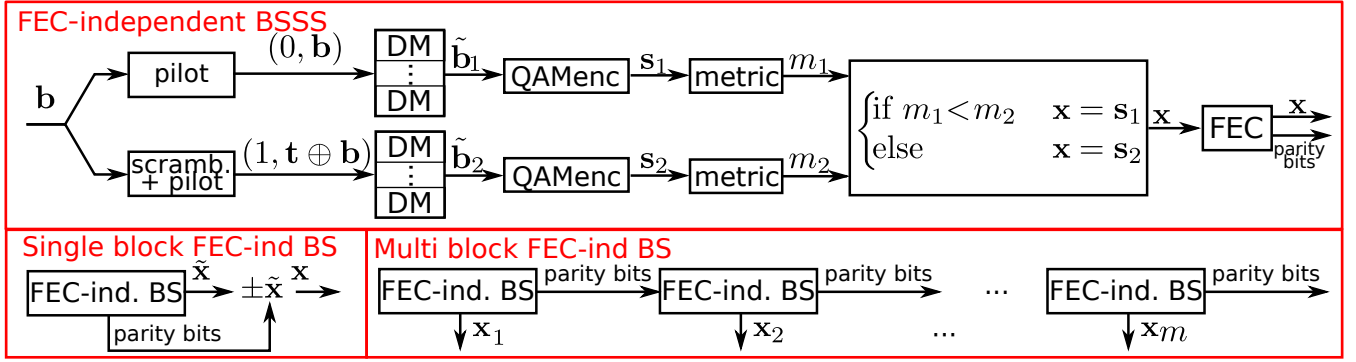


Figure 9. FEC-independent BS sequence selection (top) with single block (SB) (bottom left) and multi block (MB) (bottom right) implementations.

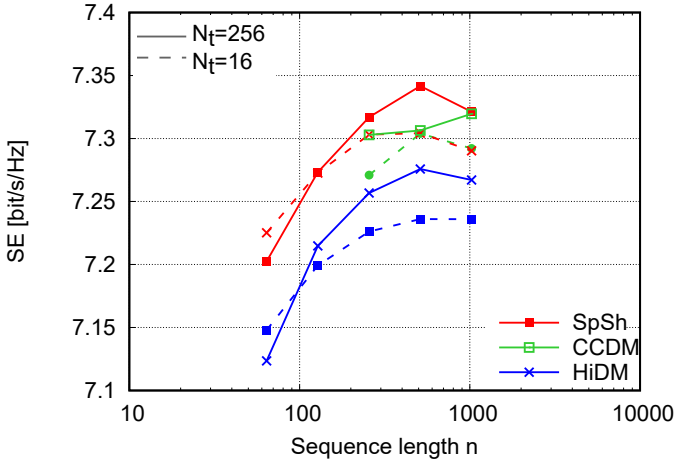


Figure 10. Performance of BS versus n .

In this Section, we add a CPR at the receiver side, implemented with the blind phase search (BPS) algorithm with 64 test angles and with a window of 281 symbols (140 on each side), previously optimized to obtain the best performance [20], [40].¹³ Furthermore, we modify the metric to measure the remaining nonlinear interference after the CPR, which is obtained by removing, for each received symbol of the tested sequence, the average phase rotation induced by nonlinear propagation over the surrounding window of 281 symbols. Figure 12 shows the peak SE (at optimal launch power) versus number of tested sequences when the CPR is included (solid) or not (dashed), with the BS approach and $n = 512$. The baseline performance without sequence selection improves significantly for i.i.d. MB-distributed symbols (whose intensity fluctuations cause a relevant nonlinear phase noise that can be mitigated by the CPR), whereas it does not improve or has a small improvement when a short-block-length DM is used (which already produces signals with less intensity fluctuations)—for more details about this refer to [20]. Conversely, the figure shows that sequence selection is able to provide approximately the same gain when CPR is included or not, in all cases. Overall, this important result implies that the nonlinear shaping gain provided by sequence selection remains

¹³For the sake of simplicity, we do not include laser phase noise in the system. However, we expect the overall result not to change, as in [20].

when CPR is included, differently from the nonlinear shaping gain obtained with short block length DM.

V. CONCLUSION

In this work the concept of nonlinear probabilistic constellation shaping was discussed. In a nutshell, nonlinear probabilistic shaping aims at improving the performance of a fiber optic communication system by encoding information onto the symbols of a QAM constellation in a smart way, taking into account the interaction of adjacent symbols in all possible dimensions (time, quadratures and polarizations). Sequence selection was used to assess the potential of nonlinear probabilistic shaping and address its implementation.

Sequence selection can be seen as a *generalization* of conventional probabilistic shaping in the absence of a priori knowledge about (i) optimal distribution, (ii) features or characteristics of a good shaping, and (iii) optimal bit-to-symbol mapping rules. Basically, sequence selection produces properly shaped sequences of symbols, starting from symbols generated by any source, referred to as *unbiased* source, and using a proper performance metric. Using some theoretical bounds based on sequence selection, we have drawn some important conclusions about nonlinear probabilistic shaping: (i) if the unbiased source is already optimized to minimize the intensity fluctuations of the signal (such as with short-block-length PAS), a further optimization of the transmitted sequences based on a sign-independent metric does not provide any additional improvement; (ii) full shaping of both amplitudes and signs achieves the best performance (with a gain of about 0.13 bits/s/Hz in a typical scenario; (iii) nearly the same performance can be achieved by shaping only the amplitudes, provided that the amplitudes are shaped depending on the values taken by the signs (i.e., by using a sign-dependent metric for sequence selection). Furthermore, we have shown that the optimal shaping does not depend critically on system parameters such as the baud rate and number of spans. In fact, a lower but still relevant gain can be obtained if those parameters are changed (within a reasonable range) without reoptimizing the shaping, allowing for a good amount of flexibility in the system optimization.

Different techniques for the practical implementation of sequence selection have been discussed, highlighting their advantages and disadvantages. The bit scrambling (BS) sequence

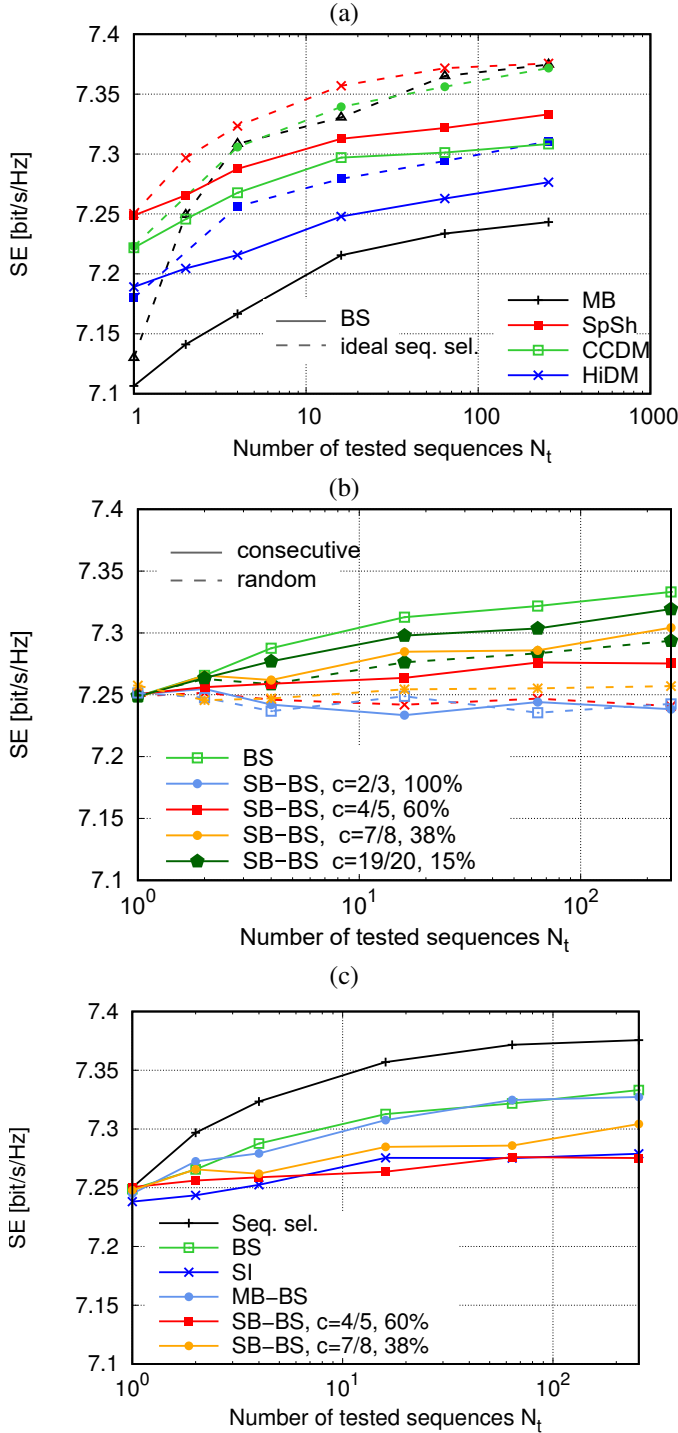


Figure 11. Performance of different sequence selection techniques for a fixed blocklength $n = 512$: (a) BS (solid) and ideal (dashed) sequence selection combined with different PAS schemes; (b) SB-BS with SpSh-based PAS and different allocation of parity bits (solid: consecutive, dashed: random); (c) all techniques compared (with SpSh-based PAS).

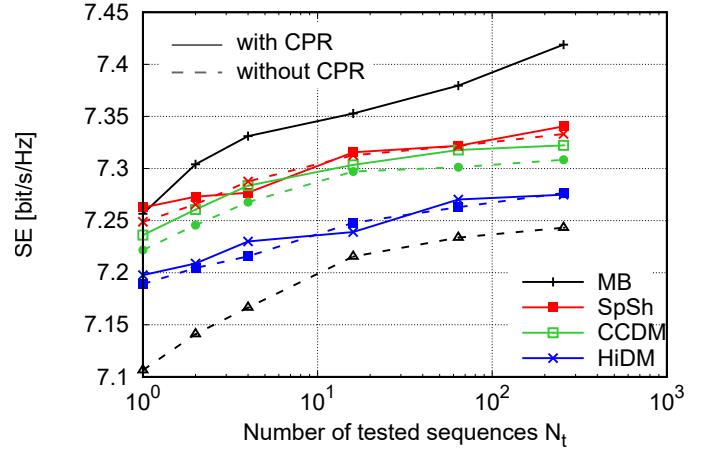


Figure 12. Impact of CPR on the performance of BS combined with different PAS schemes.

selection allows to obtain good nonlinear shaping gain, but has some issues related to the interaction with FEC. These issues can be overcome with the symbol interleaving (SI) approach, which, however, significantly hampers its performance. Therefore, we proposed two variations of BS for a FEC-independent approach: the single-block BS (SB-BS) and the multi-block BS (MB-BS). On the one hand, the SB-BS is a straightforward variation of BS, which entails only a limited performance degradation compared to BS when combined with a high-rate FEC; on the other hand, the MB-BS approach concatenates several BS blocks and is able to achieve the same performance as BS, regardless of the FEC rate, at the expense of increased latency.

The main issue affecting all sequence selection implementations and preventing their actual implementation is the complexity of the metric. Indeed, the metric should be evaluated for each test sequence, and the number of test sequences N_t should be large enough to ensure sufficiently good performance. Unfortunately, low complexity metrics, e.g., the EDI, cannot grant a good gain, when a good unbiased source is used. In this manuscript, we considered a complex metric based on the split-step Fourier method to accurately evaluate the nonlinear interference generated by each sequence. This approach, though too complex for a practical implementation, allowed us to perform this study and draw several interesting conclusions and guidelines about the implementation of sequence selection. However, the adopted metric provides an accurate estimation of the different nonlinear interference affecting each symbol of the sequence, which is a much more detailed knowledge than the one actually needed for an efficient selection. In fact, a simpler metric able to *rank* the sequences according to their *average* nonlinear interference would be sufficient to obtain the same performance. The design of such a low-complexity metric is left for a future work.

Finally, we have evaluated the performance of sequence selection when carrier phase recovery (CPR) is included in the system. Indeed, CPR is always present in practical systems and can already compensate for part of the nonlinearity, often reducing (or even eliminating) the additional improvement

achievable with other mitigation methods, such as short-block-length PAS. Conversely, we showed in this manuscript that the nonlinear shaping gain provided by sequence selection remains almost unchanged when CPR is included in the system. This result encourages the use of sequence selection for nonlinear constellation shaping.

ACKNOWLEDGEMENT

This work was partially supported by the European Union under the Italian National Recovery and Resilience Plan (NRRP) of NextGenerationEU, partnership on “Telecommunications of the Future” (PE00000001 - program “RESTART”).

REFERENCES

- [1] S. Civeili, E. Forestieri, and M. Secondini, “Probabilistic shaping methods for linear and nonlinear channels,” in *Proc. Optical Fiber Commun. Conf. (OFC)*, pp. Th3E–5, Optica Publishing Group, 2023.
- [2] S. Civeili, E. Forestieri, and M. Secondini, “Practical implementation of sequence selection for nonlinear probabilistic shaping,” in *Proc. Optical Fiber Commun. Conf. (OFC)*, pp. Th3E–2, Optica Publishing Group, 2023.
- [3] C. E. Shannon, “A mathematical theory of communication,” *Bell System Tech. J.*, vol. 27, pp. 379–423/623–656, July/Oct. 1948.
- [4] C. E. Shannon, “Communication in the presence of noise,” *Proceedings of the IRE*, vol. 37, no. 1, pp. 10–21, 1949.
- [5] A. R. Calderbank and L. H. Ozarow, “Nonequiprobable signaling on the gaussian channel,” *IEEE Trans. Inf. Theory*, vol. 36, no. 4, pp. 726–740, 1990.
- [6] F. R. Kschischang and S. Pasupathy, “Optimal nonuniform signaling for Gaussian channels,” *IEEE Trans. Inf. Theory*, vol. 39, no. 3, pp. 913–929, 1993.
- [7] G. Böcherer, F. Steiner, and P. Schulte, “Bandwidth efficient and rate-matched low-density parity-check coded modulation,” *IEEE Trans. Commun.*, vol. 63, no. 12, pp. 4651–4665, 2015.
- [8] F. Buchali, F. Steiner, G. Böcherer, L. Schmalen, P. Schulte, and W. Idler, “Rate adaptation and reach increase by probabilistically shaped 64-QAM: An experimental demonstration,” *J. Lightwave Technol.*, vol. 34, no. 7, pp. 1599–1609, 2016.
- [9] J. Cho and P. J. Winzer, “Probabilistic constellation shaping for optical fiber communications,” *J. Lightwave Technol.*, vol. 37, no. 6, pp. 1590–1607, 2019.
- [10] P. Schulte and G. Böcherer, “Constant composition distribution matching,” *IEEE Trans. Inf. Theory*, vol. 62, no. 1, pp. 430–434, 2016.
- [11] Y. C. Gültekin, T. Fehenberger, A. Alvarado, and F. M. Willems, “Probabilistic shaping for finite blocklengths: Distribution matching and sphere shaping,” *Entropy*, vol. 22, no. 5, p. 581, 2020.
- [12] T. Yoshida, M. Karlsson, and E. Agrell, “Hierarchical distribution matching for probabilistically shaped coded modulation,” *J. Lightwave Technol.*, vol. 37, no. 6, pp. 1579–1589, 2019.
- [13] S. Civeili and M. Secondini, “Hierarchical distribution matching for probabilistic amplitude shaping,” *Entropy*, vol. 22, no. 9, p. 958, 2020.
- [14] M. Secondini and E. Forestieri, “Scope and limitations of the nonlinear Shannon limit,” *J. Lightwave Technol.*, vol. 35, pp. 893–902, Feb. 2017.
- [15] O. Geller, R. Dar, M. Feder, and M. Shtaf, “A shaping algorithm for mitigating inter-channel nonlinear phase-noise in nonlinear fiber systems,” *J. Lightwave Technol.*, vol. 34, pp. 3884–3889, Aug. 2016.
- [16] T. Fehenberger, A. Alvarado, G. Böcherer, and N. Hanik, “On probabilistic shaping of quadrature amplitude modulation for the nonlinear fiber channel,” *J. Lightwave Technol.*, vol. 34, pp. 5063–5073, Nov. 2016.
- [17] J. Cho, X. Chen, G. Raybon, D. Che, E. Burrows, S. Olsson, and R. Tkach, “Shaping lightwaves in time and frequency for optical fiber communication,” *Nature communications*, vol. 13, no. 1, pp. 1–11, 2022.
- [18] S. Civeili, E. Forestieri, A. Lotsmanov, D. Razdoburdin, and M. Secondini, “A sequence selection bound for the capacity of the nonlinear fiber channel,” in *Proc. European Conf. Optical Commun. (ECOC)*, pp. 1–4, IEEE, 2021.
- [19] M. Secondini, S. Civeili, E. Forestieri, and L. Z. Khan, “New lower bounds on the capacity of optical fiber channels via optimized shaping and detection,” *J. Lightwave Technol.*, vol. 40, no. 10, pp. 3197–3209, 2022.
- [20] S. Civeili, E. Parente, E. Forestieri, and M. Secondini, “On the nonlinear shaping gain with probabilistic shaping and carrier phase recovery,” *J. Lightwave Technol.*, 2023.
- [21] A. Alvarado, T. Fehenberger, B. Chen, and F. M. Willems, “Achievable information rates for fiber optics: Applications and computations,” *J. Lightwave Technol.*, vol. 36, no. 2, pp. 424–439, 2018.
- [22] T. Fehenberger, D. S. Millar, T. Koike-Akino, K. Kojima, and K. Parsons, “Multiset-partition distribution matching,” *IEEE Trans. Commun.*, vol. 67, no. 3, pp. 1885–1893, 2018.
- [23] T. M. Cover and J. A. Thomas, *Elements of Information Theory*. Hoboken, NJ: Wiley, 2nd ed., 2006.
- [24] Y. C. Gültekin, W. J. van Houtum, S. Şerbetli, and F. M. Willems, “Constellation shaping for IEEE 802.11,” in *2017 IEEE 28th Annual International Symposium on Personal, Indoor, and Mobile Radio Communications (PIMRC)*, pp. 1–7, IEEE, 2017.
- [25] Y. Gültekin, W. van Houtum, and F. Willems, “On constellation shaping for short block lengths,” in *2018 Symposium on Information Theory and Signal Processing in the Benelux (SITB 2018)*, pp. 86–96, University of Twente, 2018.
- [26] Y. C. Gültekin, F. M. Willems, W. J. van Houtum, and S. Şerbetli, “Approximate enumerative sphere shaping,” in *Proc. IEEE Symposium on Information Theory*, pp. 676–680, IEEE, 2018.
- [27] S. Civeili and M. Secondini, “Hierarchical distribution matching: a versatile tool for probabilistic shaping,” in *Proc. Optical Fiber Commun. Conf. (OFC)*, p. Th1G.4, Optical Society of America, 2020.
- [28] A. Amari, S. Goossens, Y. C. Gültekin, O. Vassilieva, I. Kim, T. Ikeuchi, C. M. Okonkwo, F. M. Willems, and A. Alvarado, “Introducing enumerative sphere shaping for optical communication systems with short blocklengths,” *J. Lightwave Technol.*, vol. 37, no. 23, pp. 5926–5936, 2019.
- [29] T. Fehenberger, H. Griesser, and J.-P. Elbers, “Mitigating fiber nonlinearities by short-length probabilistic shaping,” in *Proc. Optical Fiber Commun. Conf. (OFC)*, pp. Th1I–2, Optical Society of America, 2020.
- [30] R. R. Borujeny and F. R. Kschischang, “Why constant-composition codes reduce nonlinear interference noise,” *J. Lightwave Technol.*, 2023.
- [31] Y. C. Gültekin, A. Alvarado, O. Vassilieva, I. Kim, P. Palacharla, C. M. Okonkwo, and F. M. Willems, “Mitigating nonlinear interference by limiting energy variations in sphere shaping,” in *Proc. Optical Fiber Commun. Conf. (OFC)*, pp. Th3F–2, Optica Publishing Group, 2022.
- [32] Y. C. Gültekin, A. Alvarado, O. Vassilieva, I. Kim, P. Palacharla, C. M. Okonkwo, and F. M. Willems, “Kurtosis-limited sphere shaping for nonlinear interference noise reduction in optical channels,” *J. Lightwave Technol.*, vol. 40, no. 1, pp. 101–112, 2021.
- [33] K. Wu, G. Liga, A. Sheikh, F. M. Willems, and A. Alvarado, “Temporal energy analysis of symbol sequences for fiber nonlinear interference modelling via energy dispersion index,” *J. Lightwave Technol.*, vol. 39, no. 18, pp. 5766–5782, 2021.
- [34] K. Wu, G. Liga, Y. C. Gültekin, and A. Alvarado, “Exponentially-weighted energy dispersion index for the nonlinear interference analysis of finite-blocklength shaping,” in *Proc. European Conf. Optical Commun. (ECOC)*, IEEE, 2021.
- [35] M. T. Askari, L. Lampe, and J. Mitra, “Probabilistic amplitude shaping and nonlinearity tolerance: Analysis and sequence selection method,” *J. Lightwave Technol.*, 2023.
- [36] K. Wu, G. Liga, A. Sheikh, Y. C. Gültekin, F. M. Willems, and A. Alvarado, “List-encoding CCDDM: A nonlinearity-tolerant shaper aided by energy dispersion index,” *J. Lightwave Technol.*, vol. 40, no. 4, pp. 1064–1071, 2022.
- [37] M. T. Askari, L. Lampe, and J. Mitra, “Nonlinearity tolerant shaping with sequence selection,” in *Proc. European Conf. Optical Commun. (ECOC)*, IEEE, 2022.
- [38] G. Böcherer and R. Mathar, “Operating LDPC codes with zero shaping gap,” in *2011 IEEE Information Theory Workshop*, pp. 330–334, IEEE, 2011.
- [39] S. Civeili, E. Forestieri, and M. Secondini, “Interplay of probabilistic shaping and carrier phase recovery for nonlinearity mitigation,” in *Proc. European Conf. Optical Commun. (ECOC)*, IEEE, 2020.
- [40] T. Pfau, S. Hoffmann, and R. Noé, “Hardware-efficient coherent digital receiver concept with feedforward carrier recovery for m -qam constellations,” *J. Lightwave Technol.*, vol. 27, no. 8, pp. 989–999, 2009.